RSC Advances




ROYAL SOCIETY OF CHEMISTRY

www.rsc.org/advances

Journal Name

ARTICLE

# Photophysical properties of quinoxaline-fused [7]carbohelicene derivatives

Received 00th January 20xx,
Accepted 00th January 20xx

DOI: 10.1039/x0xx00000x

www.rsc.org/

Chunyu Liu,[a] Yanling Si,[b] Xiumei Pan[a,*] and Guochun Yang[a,*]

Helicene and its derivatives have received much attention as the candidates of organic photoelectronic material. Recently, novel quinoxaline-fused [7]carbohelicene derivatives exhibit unique structural and photophysical properties, especially in the crystal states. However, their structure-property relationships have not been fully understood from the micromechanism, which is also important to further improve their performance. Here, the electronic transition, electronic circular dichroism (CD), second-order nonlinear optical (NLO) response and charge transport properties of five quinoxaline-fused [7]carbohelicene derivatives have been investigated based on density functional theory calculations. The experimental UV-Vis/CD spectra of the studied compounds were well reproduced by our calculations. Thus, we can assign their electron transition properties and absolution configurations (ACs) with high confidence. It is found that CD bands of quinoxaline-fused [7]carbohelicene derivatives mainly originate from exciton coupling between quinoxaline, phenyl or 4-methoxyphenyl and [7]carbohelicene, which is in sharp contrast to [7]carbohelicene. More interestingly, these derivatives possess large first hyperpolarizability values. For example, the $\beta_{HRS}$ value of compound **6** is $32.96 \times 10^{-30}$ esu, which is about 190 times larger than that of the organic urea molecule. The bandwidth of valence band of compound **2** is comparable to that of conduction band and slightly larger than that of tris(8-hydroxyquinolinato)aluminium. This means that compound **2** is the potential candidate as ambipolar charge transport material.

## Introduction

Chirality is not only vital to our life but also plays an important role in material science.[1-5] Thus, much affords have been made towards controlling and understanding chirality in chemical synthesis and material design. Helicenes are polycyclic aromatic compounds with screw-shaped skeletons formed by ortho-fused benzene or other aromatic rings.[6-9] Steric hindrance interaction between terminal aromatic rings endows helicenes with helical chirality. As a consequence, helicenes exhibit high optical rotation and circular dichroism values in the visible region.[10-17] More interesting, the dissymmetric backbone makes helicenes and their derivatives applications in many fields (e.g. asymmetric catalysis,[18-21] liquid crystal molecules,[22] enantioselective fluorescent sensors,[23] rotors,[24] nonlinear optics,[25-27] molecular recognition[28-31] and organic electronics[32-36]).

Among the carbohelicene family, [7]carbohelicene is the most interesting member due to its high optical stability (racemization barrier is 40.5 kcal/mol),[37, 38] easy decoration and functionization, and distinguishable photophysical properties.[37, 39, 40] For example, [7]carbohelicene can function as a "molecular tweezer"[41-43] of some metallic cations. Fascinating chiroptical properties has been observed by introducing silver(I) ion moieties into [7]carbohelicene.[37] Facchetti et al. reported that tetrathia-[7]-helicene derivatives act as *p*-type semiconductors with high carrier mobility in organic thin-film transistors.[44, 45] 2,12-dihexyl-2,12-diaza[7]helicene can serve as a deep-blue dopant emitter in an organic light-emitting diode.[46] Moreover, [7]carbohelicene can be easily functionalized by varying the substituents. Specifically, the photophysical properties of tetrathia-[7]-helicene can greatly modulated by decorating the two terminal thiophene rings.[47,48] Specifically, novel organometallic Ru(II) and Fe(II) complexes with tetrathia-[7]-helicene have been synthesized. Studies show that tetrathia-[7]-helicene and their Ru(II) and Fe(II) complexes are good candidates for second-order NLO materials.[27, 49]

Quinoxaline (i.e., benzopyrazine) can be easily synthesized from diketones and diamines.[50] Quinoxaline has the strong electron-withdrawing ability, which originates from the two unsaturated nitrogen atoms in the pyrazine ring. Due to the highly polarized nature of the imine units, quinoxalines are extensively used as light-emitting and electron-transporting materials.[51] Moreover, incorporation of quinoxaline unit might be in favour of forming CH···N interactions and influence the crystal packing.[52] As a consequence, the quinoxaline units are expected to enhance the

[a] Faculty of Chemistry, Northeast NormalUniversity, Changchun, 130024 Jilin, China. E-mail: panxm460@nenu.edu.cn;yanggc468@nenu.edu.cn
[b] College of Resource and Environmental Science, Jilin Agricultural University,Changchun, Jilin 130118, P. R. China

† Fotnotes relating to the title and/or authors should appear here.

Electronic Supplementary Information (ESI) available: The simulated UV-Vis spectra and CD spectra for the different functionals; the compared bond-length between calculation and experimental measurement; the calculated excitation energies, oscillator and rotational strengths of the 60 lowest energy electronic excitations; molecular orbitals involved into the main electronic transition. See DOI: 10.1039/x0xx00000x

luminous efficiency and to control the packing structures in the crystal. Recently, Sakai et al. synthesized a series of quinoxaline-fused [7]carbohelicenes (Fig. 1). It is found that involving quinoxaline into [7]carbohelicene greatly enhances the fluorescence quantum yields. Specifically, the fluorescence quantum yield of compound **2** is about four times larger than that of compound **1**. Notably, quinoxaline-fused [7]carbohelicene derivatives can form unique crystal packing. For example, compound **2** forms racemic crystal packing through intermolecular interactions (π···π, CH···N and CH···π). One-dimensional helical columns were firstly observed, which contains the racemic compound **4**. This helical columnar structure contains both π–π stacking and CH···N interaction, which is in sharp contrast to the packing motif of the corresponding enantiomer. Moreover, the excimer-like delocalized excited state was clearly observed by time-resolved fluorescence measurements.[51]

It is well known that macroscopic properties strongly correlate with the microcosmic electron structures, especially for the electron transition properties upon exaction. As far as we known, only frontier molecular orbital levels of quinoxaline-fused [7]carbohelicene derivatives were studied at B3LYP/6-31G* level of theory.[51] By all appearance, there is necessary to systemically investigate their photophysical properties and establish the structure-property relationship at the quantum chemistry level of theory. The main aim of the current investigation was (i) to evaluate the reliability of TDDFT in simulating the UV-Vis/CD spectra of the studied compounds, (ii) to assign their absolute configurations (ACs), (iii) to describe their electronic transition properties and chiroptical origions, (iv) to investigate their NLO and charge transport properties and find their potential application in the materials science field.

## 2. Computational details

Geometrical optimization of the studied compounds was carried out using the B3LYP[53] functional as implemented in the Gaussian 09 computational program suite.[54] During the process of optimization, there are no symmetry or internal coordination constraints. The B3LYP functional is a combination of Becke's three-parameter hybrid exchange functional[53, 55] and the Lee–Yang–Parr[56] correlation functional. Basis sets of 6-31G(d,p) for C, O, N, and H atoms were applied. The harmonic vibration calculation was used to confirm their minimum.

To investigate linear and chiroptical properties, the electron excitation energies, oscillator strengths, and rotational strengths for the studied compounds were calculated at the TDB3LYP/6-31+G(d) level of theory. Both length and velocity representations were used to obtain rotational strengths. It is noted that the velocity-gauge representation of the dipole operator is gauge origin independent. Gaussian bandshapes[57] with a bandwidth of 0.12 eV were used to compare the calculated UV–Vis/CD spectra with experimental ones. The effect of different basis sets and DFT functionals on UV-Vis/CD spectra was also tested. To test the effect of solvent on the CD spectra, the LR-PCM model[58, 59] was utilized as implemented in Gaussian 09. The solvent tetrahydrofuran (THF) was treated as a continuous dielectric environment with a dielectric constant of 7.4257.

The first hyperpolarizability was calculated as performed in the Gaussian 09 program package. It is noted that hyper-Rayleigh scattering (HRS) was used to determine the second-order nonlinear optical response (NLO) properties. In the case of plane-polarized incident light and observation made perpendicular to the propagation plane without polarization analysis of the scattered beam, the second-order NLO response that can be extracted from HRS data can be described as:[60, 61]

$$\beta_{HRS}(0;0,0) = \sqrt{\{\langle\beta_{ZZZ}^2\rangle + \langle\beta_{XZZ}^2\rangle\}} \quad (1)$$

$\langle\beta_{ZZZ}^2\rangle$ and $\langle\beta_{XZZ}^2\rangle$ correspond to the orientational average of the β tensor without assuming Kleinman's conditions.[62] Here, we only concerned the static first hyperpolarizability. So, the frequency value in Eq (1) was set to zero.

To investigate the electronic properties in bulk, electronic band structure calculation was performed by a DFT method as implemented in the Vienna Ab-initio Simulation Package (VASP)[63, 64] with Perdew–Burke–Emzerhof (PBE) for the exchange correlation functionals and a plane-wave basis set with an energy cut-off of 400 eV. The Monkhorst–Pack scheme was used to sample the Brillouin zone with grid spacing of 2π × 0.04 Å$^{-1}$.

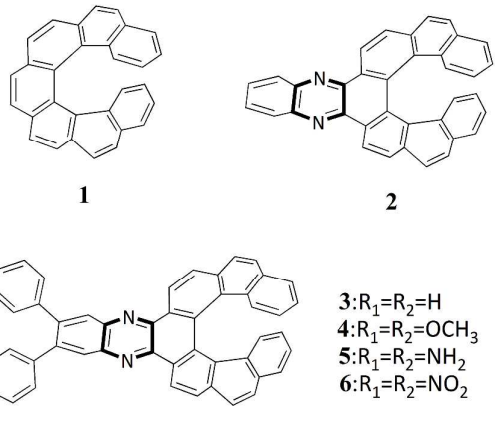


**Fig. 1** Chemical structures of the studied compounds **1–6**.

## 3. Results and discussion

### 3.1. Molecular structures

In this paper, five quinoxaline-fused [7]carbohelicene derivatives were investigated (Fig. 1). To test the influence of quinoxaline on the electronic property, [7]carbohelicene was also included. Compounds **2-4** have been synthesized and characterized by X-ray crystallography.[51] Compounds **5** and **6** were designed to investigate the charge transfer cooperativity and find the effective way to enhance their NLO response. The geometric structures of studied compounds were fully optimized without any symmetry constraint at the B3LYP/6-31G(d,p) level of theory. The absence of the imaginary frequencies confirms that our optimized structures are minima. It is noted that the optimized geometries of studied compounds have $C_1$ symmetry. Here, compound **4** taken as an example to test our adopted method, its main structural parameters were well reproduced by our calculation (Table S1).

Thus, the adopted basis set and functional are suitable to describe molecular structures for the studied compounds.

### 3.2. The selection of the basis sets and functionals for the studied compounds

Time-dependent density functional theory (TDDFT) method has extensively been employed to investigate the electronic transition properties[65-70] and chiroptical properties[71-80] of diverse compounds. In general, electronic transition properties are sensitive to basis sets[81-84] and DFT functionals,[85-93] especially for CD calculation. For our studied compounds, Sakai et al. only calculated their frontier molecular orbital level at B3LYP/6-31G* level.[51] Their electronic transition properties have not been systematically studied thus far. As a consequence, five Pople's basis sets: 6-31G(d), 6-31+G(d), 6-31++G(d,p), 6-311++G(d,p), and 6-311++G(2d,2p) were selected to assess the influence of the basis set extension on the absorption wavelengths by using B3LYP functional, which is the most popular functional for organic compounds. For the compound **2**, an intense absorption band at 276 nm and three moderately intense absorption bands at 332, 366 and 427 nm were observed.[51] The computed absorption wavelengths at the different basis sets level are listed in Table S2. It is noted that the four observed bands are well reproduced by our calculations. Moreover, the difference of absorption wavelength between the largest basis set and the smallest basis set is within 8 nm, which means the effect of basis set size on the calculated absorption wavelengths is negligible. Previous study shows that diffuse functions play a vital role in obtaining the accurate absorption wavelength and describing the electronic transition property.[94] Thus, 6-31+G(d) basis set was used in the following calculation. Subsequently, five DFT functionals: B3PW91,[95-97] M06-2X,[98, 99] BH&HLYP,[100, 101] PBE0,[102, 103] and B3LYP,[53] were selected to evaluate the influence of these DFT functionals on the absorption wavelengths. The simulated UV-Vis and CD spectra using these functionals along the experimental ones were given in Fig. S1. The results show that the computed absorption wavelengths strongly depend on the used functionals. Specifically**,** the M06-2X and BH&HLYP functionals could not reproduce the experimental absorption band at about 427 nm. The same trend was also observed in simulated CD spectra. This observation might result from the larger energy gaps of the M06-2X and BH&HLYP functionals (Table S3). However, both band positions and shapes of the B3LYP, B3PW91 and PBE0 functionals are similar, which might be due to their similar HF exchange fraction. It is well known that conventional TDDFT methods usually underestimate the charge-transfer excitations due to the semi-local exchange-correlation effects. Studies have shown that the range-separated functional (e.g. LC-BLYP and LC-PBE) can give correct localization, HOMO-LUMO gaps, and ionization/electron affinity energies. For example, the range-separated functionals have successfully described the optoelectronic and excitonic properties of oligoacenes.[104, 105] Thus, we also selected the LC-BLYP functional to calculate the electronic excitation property for compound **2**. The experimental spectra of compound **2** are not well reproduced by the LC-BLYP functional (Fig. S1). Overall, the results computed with the B3LYP functional are much closer to experimental ones. Thus, the B3LYP functional combined with 6-31+G(d) basis set were employed in the following calculations.

### 3.3. UV-Vis and CD spectra

In general, the more experimental bands are involved in the theoretical calculation, the more reliable is for the assignment of the AC.[106] Thus, the 60 lowest energies for the studied compounds were calculated at the TDB3LYP/6-31+G(d) level, which cover the range of experimental measurement (Table S4). The calculated absorption wavelengths, oscillator strengths, and major contributions of the studied compounds, as compared to experimental values, were summarized in Table 1 and Table S5. The simulated UV-Vis/CD spectra were shown in Fig. 2 along with the experimental spectra. Notably, the simulated UV–Vis/CD spectra are in reasonably good agreement with the experimental ones, not only for the relative peak intensities but also the band positions. Moreover, the values of the rotational strengths calculated using the length and velocity gauge representation of the electric dipole operator are close to each other. (Table S4, Supporting Information). Thus, our adopted method can reliably describe the electron transition property and assign the ACs of the quinoxaline-fused [7]carbohelicene derivatives with high confidence. The CD spectra might be sensitive to the solvent.[107] The geometries of the studied compounds are re-optimized to test the influence of THF solvent under the PCM model. Then, their solution UV-Vis/CD spectra were also re-calculated based on PCM structures (Fig. S2). It is found that the shape of solution UV-Vis/CD spectra are nearly same as the gas phase ones except the slightly hypsochromic shift. This indicates that the influence of the solvent is negligible for the studied compounds.

**Table 1.** Computed absorption wavelengths (λ in nm) as compared to experimental data (in parentheses), oscillator strengths (*f*), and major contribution for the compound **2** at B3LYP/6-31+G(d) level of theory.

| Band | λ | f | Major contribution |
|---|---|---|---|
| Band 1 | 282.49(276) | 0.782 | HOMO-4→LUMO+2 (42%)<br>HOMO→LUMO+4 (14%) |
| Band 2 | 316.45(332) | 0.220 | HOMO-6→LUMO (77%)<br>HOMO-4→LUMO+2 (9%) |
| Band 3 | 346.13(366) | 0.207 | HOMO→LUMO+2 (37%)<br>HOMO-1→LUMO+1 (22%) |
| Band 4 | 424.85(427) | 0.190 | HOMO-1→LUMO (85%)<br>HOMO→LUMO+2 (12%) |

The molecular orbitals (MO) involved in the main electronic transitions for the studied compounds **1–4** are shown in Fig. 3 and Fig. S3, respectively. Compound **1** ([7]carbohelicene) exhibits an intense absorption band at 274 nm and two relatively weak absorption band at 312 and 374 nm. Its main electron transition characteristics can be described as $\pi$-$\pi^*$, as characterized by these orbitals are $\pi$ symmetry features. However, compound **2** exhibits four main absorption bands (282, 316, 346, and 425 nm). Notably, the main absorption bands of compound **2** are red-shifted compared with those of compound **1**, which are also agreement with the experimental observations.[51] Quinoxaline is an electron-acceptor group.[51] In general, the electron-acceptor group mainly

modulates the LUMO energy level. As a consequence, LUMO energy of compound **2** is much lower than that of compound **1** (Table S6), which leads to the smaller energy gap (*Eg*) for compound **2**. Moreover, the main electron transitions characters are of charge transfer from quinoxaline to [7]carbohelicene and *vice versa* (Fig. 3). On the basis of above analysis, it is found that involvement of quinoxaline unit not only modulates the electron absorption wavelength but also alter the electron transition property. Compounds **3** and **4** also exhibit four absorption bands, which is similar to those of compound **2.** In other words, the substituent effect of phenyl or 4-methoxyphenyl group on the UV–Vis spectra of compound **2** is not great. It is noted that some of the molecular orbitals involved in these transitions partially located on the phenyl or 4-methoxyphenyl group.

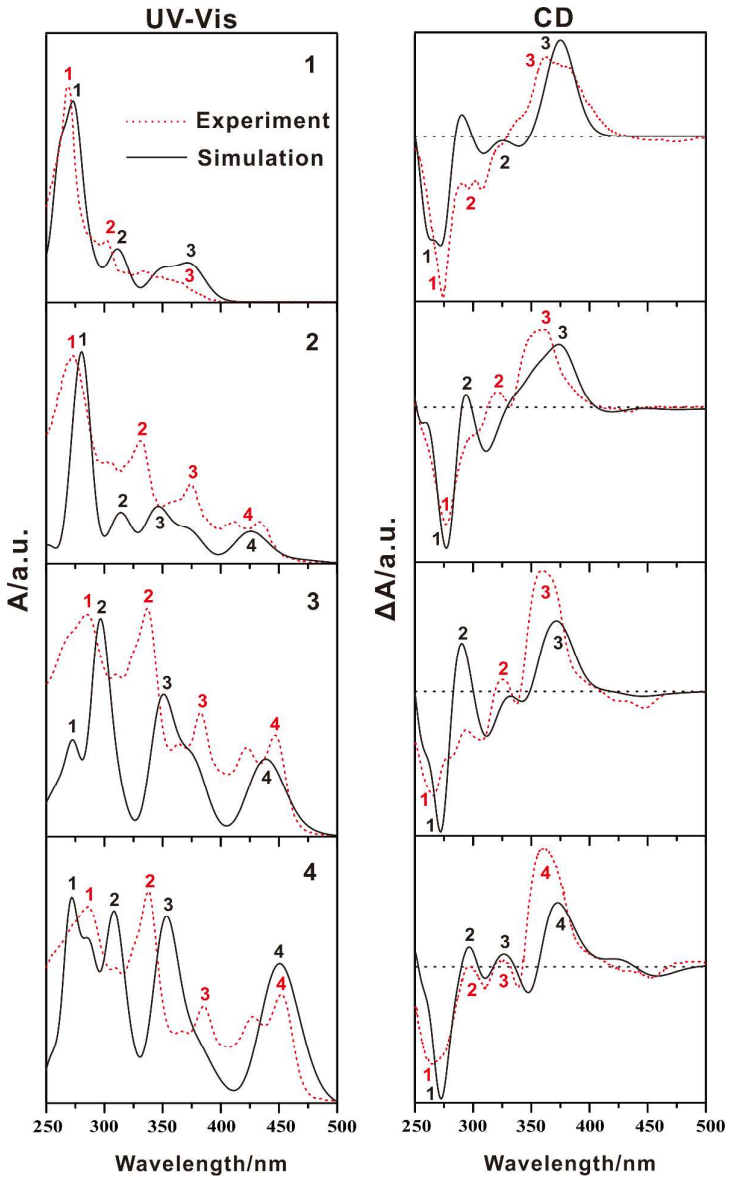


**Fig. 2** Calculated UV-Vis (left) and CD (right) spectra in gas phase of **1**, **2**, **3** and **4** at the TDB3LYP/6-31+G(d) level of theory along with the experimental spectra (red dashed line). Data to prepare the experimental spectra was taken from ref. 51.

Journal Name

ARTICLE

Although the CD spectra of quinoxaline-fused [7]carbohelicene deriveeatives (compounds **2-4**) are similar to those of [7]carbohelicene (compound **1**), there is a slight difference between them. Specifically, compound **1** exhibits a negative Cotton band around 300 nm (labeled as band 2), while this band becomes positive in compounds **2-4**. These indicate that CD spectra are sensitive to molecular structures. It should be noted that the calculated relative peak intensities around 300 nm (labeled as band 2) of compounds **1-3** are slightly different from the experimental ones. To further understand the chiral origins of the studied compounds, their corresponding molecular orbitals are shown in Fig. S4. The analysis shows there is common character of chiral origins for quinoxaline-fused [7]carbohelicene derivatives (compounds **2-4**), which can be attributed to the exciton coupling between quinoxaline, phenyl or 4-methoxyphenyl and [7]carbohelicene, which is completely different from those of [7]carbohelicene (Fig. S4).

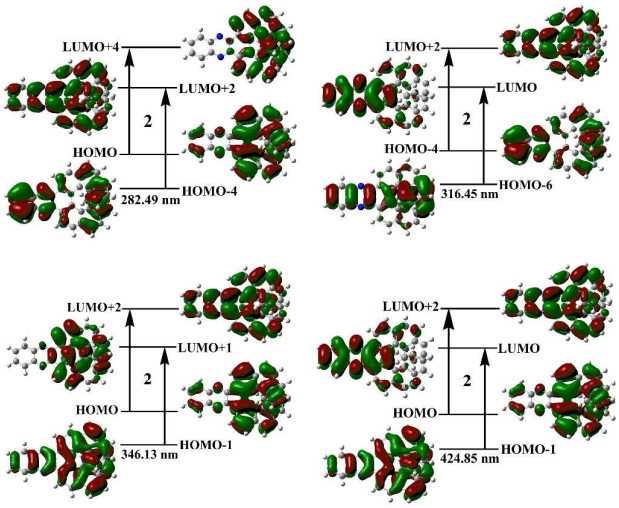


**Fig. 3** Molecular orbital isosurfaces involved in the main electron transitions of compound **2** at the TDB3LYP/6-31+G(d) level of theory.

### 3.4. Second-order nonlinear optical response (NLO) property

Chiral compounds have been viewed as a valuable alternative in the search for new second-order NLO material due to their intrinsic non-centrosymmetric structures,[108] which allows its NLO effects to be observed even in highly symmetric media.[108, 109] Based above electronic transition analysis, quinoxaline-fused [7]carbohelicene derivatives (compounds **2-4**) exhibit intramolecular charge transfer. Thus, the larger intramolecular charge transfer will come into being under the external electron field and a large NLO response could be observed. Strong electron donor ($NH_2$) or electron acceptor ($NO_2$) groups were also introduced to probe the charger transfer cooperativity and find the effective way to enhance NLO response. Recently, DFT calculations have emerged as a powerful tool for investigation and prediction of the compounds with large NLO response.[110-115] Thus, the first hyperpolarizability ($\beta_{HRS}$) values of the studied compounds were calculated at CAM-B3LYP/6-31+G(d) level and were given in Table 2. The calculated $\beta_{HRS}$ values of these studied compounds are larger than those of the typical organic NLO compounds. For example, the calculated $\beta_{HRS}$ value of compound **6** is about 8 times larger than that of the highly π-delocalized phenyliminomethyl ferrocene complex[116, 117] and 190 times larger than that of the organic urea molecule.[66, 118] Thus, the studied compounds could become excellent second-order NLO materials. The $\beta_{HRS}$ values for compounds **3-5** increase as follows: **3**<**4**<**5**, which is agreement with the trend of electron donor ability (H < $OCH_3$ < $NH_2$). However, Compound **6** has the largest $\beta_{HRS}$ value among these compounds. Thus, $NO_2$ as the terminal substitution is an effective way to enhance the NLO response. Eelectron transition analysis shows that the charge transfer from [7]carbohelicene to nitrobenzene moieties plays the key role in determining its NLO response. (Fig S3). The quinoxaline group in compound **6** acts as a bridge of charge transfer. It is noted that compound **6** has the smallest the band gaps (Table S6).

**Table 2.** The calculated first hyperpolarizability ($\beta_{HRS}$) values ($10^{-30}$ esu) of the studied compounds **3-6** at CAM-B3LYP/6-31+G(d) level of theory.

| Compound | $\beta_{HRS}$ |
|---|---|
| **3** | 4.43 |
| **4** | 10.87 |
| **5** | 20.09 |
| **6** | 32.96 |

## 3.5 Charge transport property

Recently, helicene derivatives have exhibited good and unique charge transport ability,[45, 119] which is very important for improving the performance of organic thin-film transistors and organic light emitting diodes. For example, unprecedented carrier inversion has been observation for azaboradibenzo[6]helicene. Its racemate acts as hole transport material, while the single enantiomer as electron transport material.[119] Compound contains quinoxaline group exhibits excellent electron transport ability.[120] Interesting, quinoxaline-fused [7]carbohelicene derivatives possess unique crystal

packing, as discussed in the introduction. Inspired by those, we investigate their charge transport properties by using the band model.[121, 122] From the view point of band model, the larger bandwidth is, the larger carrier mobility is.[123] It is noted that the spatial distribution of the corresponding wavefunctions is also a factor that influences the charge transport property. Here, we mainly concerned it from the band model. The calculated band structures of compounds **2** and **4** using Vienna *ab-initio* simulation package along high-symmetry directions were shown in Fig. 4 and Fig. S5. For compound **2**, the bandwidth of valence band (0.10 eV) is almost equal to that of conduction band (0.08 eV) and slightly larger than that of tris(8-hydroxyquinolinato)aluminium (AlQ). This finding can also be supported by its frontier molecular orbital. That is, HOMO is mainly localized on the [7]carbohelicene part, while LOMO sits on the quinoxaline group (Fig. 3). This is a typical feature for ambipolar charge transport material.[124, 125] Thus, compounds **2** can act as an ambipolar charge transport material. Compound **4** forms enantiomer and racemate crystals, respectively. It is found that racemte is favour of electron transport, while enantiomer is favour of ambipolar charge transport. It should be noted that the charge transport ability of compound **4** is much lower than that of compound **1**.

## 4. Conclusion

In this paper, the UV-Vis absorption spectra, CD spectra, charge transport, and second-order NLO properties of a series of quinoxaline-fused [7]carbohelicene derivatives were systemically investigated by using density functional theory. The calculated UV-Vis/CD spectra are in good agreement with the experimental ones, which can be used to assign the electron transition property and ACs with high confidence. Exciton coupling between quinoxaline, phenyl or 4-methoxyphenyl and [7]carbohelicene are mainly responsible for chiroptical origin of the quinoxaline-fused [7]carbohelicene derivatives. The charge transport abilities of the studied compounds are sensitive to not only molecular structure but also crystal packing. Compound **2** can act as an ambipolar charge transport material. In view of the first hyperpolarizability ($\beta_{HRS}$) values and intrinsic non-centrosymmetric electronic structure, the studied compounds have the potential to be excellent second-order NLO materials.

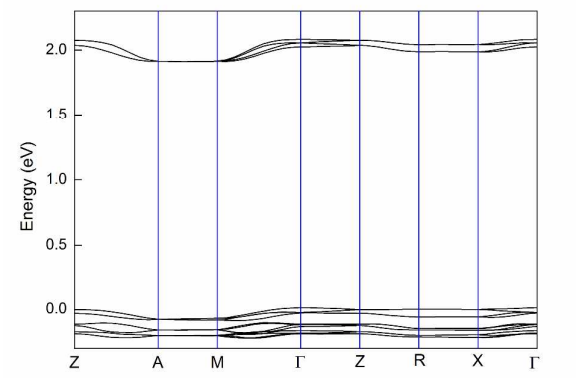


**Fig. 4** Calculated band structure of the crystal for compound **2**. The high symmetry points are Z = (0,0,0.5), A = (0.5,0.5,0.5), M = (0.5,0.5,0), Γ = (0,0,0), Z = (0,0,0.5), R = (0,0.5,0.5), X= (0,0.5,0) and Γ= (0,0,0).

## 5. Acknowledgements

The authors gratefully acknowledge the financial support from the National Natural Science Foundation of China (21377021) and the Natural Science Foundation of Jilin Province (20140101045JC and 20150101042JC).

## 6. Notes and references

1. H. Ascolani, M. W. van der Meijden, L. J. Cristina, J. E. Gayone, R. M. Kellogg, J. D. Fuhr and M. Lingenfelder, *Chem. Commun.*, 2014, **50**, 13907-13909.
2. A. Shchyrba, M. T. Nguyen, C. Wackerlin, S. Martens, S. Nowakowska, T. Ivas, J. Roose, T. Nijs, S. Boz, M. Schar, M. Stohr, C. A. Pignedoli, C. Thilgen, F. Diederich, D. Passerone and T. A. Jung, *J. Am. Chem. Soc.* , 2013, **135**, 15270-15273.
3. T. Balandina, M. W. van der Meijden, O. Ivasenko, D. Cornil, J. Cornil, R. Lazzaroni, R. M. Kellogg and S. De Feyter, *Chem. Commun.*, 2013, **49**, 2207-2209.
4. N. Saleh, B. Moore, II, M. Srebro, N. Vanthuyne, L. Toupet, J. A. Williams, C. Roussel, K. K. Deol, G. Muller, J. Autschbach and J. Crassous, *Chem. Eur. J.*, 2015, **21**, 1673-1681.
5. J. J. Xie, Y. Y. Duan and S. A. Che, *Adv. Funct. Mater.*, 2012, **22**, 3784-3792.
6. J. F. Lamère, I. Malfant, A. Sournia-Saquet, P. G. Lacroix, J. M. Fabre, L. Kaboub, T. Abbaz, A.-K. Gouasmia, I. Asselberghs and K. Clays, *Chem. Mater.*, 2007, **19**, 805-815.
7. E. Gomar-Nadal, J. Veciana, C. Rovira and D. B. Amabilino, *Adv.Mater.*, 2005, **17**, 2095-2098.
8. P. G. Lacroix, *Chem. Mater.* , 2001, **13**, 3495-3506.
9. A. Bousseksou, G. b. Molnár and G. Matouzenko, *Eur. J. Inorg. Chem.*, 2004, **2004**, 4353-4369.
10. M. J. Fuchter, M. Weimar, X. Yang, D. K. Judge and A. J. P. White, *Tetrahedron Lett.*, 2012, **53**, 1108-1111.
11. G. M. Upadhyay, H. R. Talele, S. Sahoo and A. V. Bedekar, *Tetrahedron Lett.*, 2014, **55**, 5394-5399.
12. F. Aloui, S. Moussa and B. B. Hassine, *Tetrahedron Lett.*, 2012, **53**, 3216-3219.
13. Y. Shen, H. Y. Lu and C. F. Chen, *Angew. Chem. Int. Ed.*, 2014, **53**, 4648-4651.
14. A. Ueda, H. Wasa, S. Suzuki, K. Okada, K. Sato, T. Takui and Y. Morita, *Angew. Chem. Int. Ed.*, 2012, **51**, 6691-6695.
15. S. Moussa Mel, M. Srebro, E. Anger, N. Vanthuyne, C. Roussel, C. Lescop, J. Autschbach and J. Crassous, *Chirality*, 2013, **25**, 455-465.
16. M. Gingras, *Chem. Soc. Rev.*, 2013, **42**, 968-1006.
17. C. Shen, E. Anger, M. Srebro, N. Vanthuyne, K. K. Deol, T. D. Jefferson, Jr., G. Muller, J. A. Gareth Williams, L. Toupet, C. Roussel, J. Autschbach, R. Reau and J. Crassous, *Chem. Sci.*, 2014, **5**, 1915-1927.
18. P. Aillard, A. Voituriez and A. Marinetti, *Dalton Trans.*, 2014, **43**, 15263-15278.
19. M. J. Narcis and N. Takenaka, *Eur. J. Org. Chem.*, 2014, **2014**, 21-34.
20. N. Takenaka, R. S. Sarangthem and B. Captain, *Angew. Chem. Int. Ed.*, 2008, **47**, 9708-9710.
21. K. Soai and I. Sato, *Chirality*, 2002, **14**, 548-554.
22. C. Nuckolls and T. J. Katz, *J. Am. Chem. Soc.* , 1998, **120**, 9541-9544.

23. M. T. Reetz and S. Sostmann, *Tetrahedron*, 2001, **57**, 2515-2520.
24. H. Guédouar, F. Aloui, S. Moussa, J. Marrot and B. Ben Hassine, *Tetrahedron Lett.*, 2014, **55**, 6167-6170.
25. E. Botek, B. Champagne, M. Turki and J. M. Andre, *J. Chem. Phys.*, 2004, **120**, 2042-2048.
26. T. Verbiest, S. V. Elshocht, M. Kauranen, L. Hellemans, J. Snauwaert, C. Nuckolls, T. J. Katz and A. Persoons, *Science*, 1998, **282**, 913-915.
27. C. A. Daul, I. Ciofini and V. Weber, *Int. J. Quantum. Chem.*, 2003, **91**, 297-302.
28. E. Murguly, R. McDonald and N. R. Branda, *Org. Lett.*, 2000, **2**, 3169-3172.
29. Z. An and M. Yamaguchi, *Chem. Commun.*, 2012, **48**, 7383-7385.
30. S. Honzawa, H. Okubo, S. Anzai, M. Yamaguchi, K. Tsumoto and I. Kumagai, *Bioorg. Med. Chem.*, 2002, **10**, 3213-3218.
31. H. Nakagawa, M. Yoshida, Y. Kobori and K.-i. Yamada, *Chirality*, 2003, **15**, 703-708.
32. J. Storch, J. Zadny, T. Strasak, M. Kubala, J. Sykora, M. Dusek, V. Cirkva, P. Matejka, M. Krbal and J. Vacek, *Chem. Eur. J.*, 2015, **21**, 2343-2347.
33. N. Islam and A. H. Pandith, *J. Mol. Model.*, 2014, **20**, 2535.
34. R. Hassey, E. J. Swain, N. I. Hammer, D. Venkataraman and M. D. Barnes, *Science*, 2006, **314**, 1437-1439.
35. R. Hassey, K. D. McCarthy, E. Swain, D. Basak, D. Venkataraman and M. D. Barnes, *Chirality*, 2008, **20**, 1039-1046.
36. Y. Zhou, T. Lei, L. Wang, J. Pei, Y. Cao and J. Wang, *Adv. Mater.*, 2010, **22**, 1484-1487.
37. M. J. Fuchter, J. Schaefer, D. K. Judge, B. Wardzinski, M. Weimar and I. Krossing, *Dalton Trans.*, 2012, **41**, 8238-8241.
38. J. Žádný, P. Velíšek, M. Jakubec, J. Sýkora, V. Církva and J. Storch, *Tetrahedron*, 2013, **69**, 6213-6218.
39. A. Urbano, *Angew. Chem. Int. Ed.*, 2003, **42**, 3986-3989.
40. M. C. Carreno, M. Gonzalez-Lopez and A. Urbano, *Chem. Commun.*, 2005, 611-613.
41. F.-G. Klärner and B. Kahlert, *Acc. Chem. Res.*, 2003, **36**, 919-932.
42. T. Jaunet-Lahary, D. Jacquemin, B. Legouin, J.-Y. L. Questel, J.-F. Cupif, L. Toupet, P. Uriac and J. Graton, *J. Phys. Chem. C*, 2015, **119**, 3771-3779.
43. M. Lindqvist, K. Borre, K. Axenov, B. Kotai, M. Nieger, M. Leskela, I. Papai and T. Repo, *J. Am. Chem. Soc.* , 2015, **137**, 4038-4041.
44. Y. L. Si and G. C. Yang, *J. Mater. Chem. C*, 2013, **1**, 2354-2361.
45. C. Kim, T. J. Marks, A. Facchetti, M. Schiavo, A. Bossi, S. Maiorana, E. Licandro, F. Todescato, S. Toffanin, M. Muccini, C. Graiff and A. Tiripicchio, *Org. Electron.*, 2009, **10**, 1511-1520.
46. L. Q. Shi, Z. Liu, G. F. Dong, L. Duan, Y. Qiu, J. Jia, W. Guo, D. Zhao, D. L. Cui and X. T. Tao, *Chem. Eur. J.*, 2012, **18**, 8092-8099.
47. M. Monteforte, S. Cauteruccio, S. Maiorana, T. Benincori, A. Forni, L. Raimondi, C. Graiff, A. Tiripicchio, G. R. Stephenson and E. Licandro, *Eur. J. Org. Chem.*, 2011, **2011**, 5649-5658.
48. S. Maiorana, A. Papagni, E. Licandro, R. Annunziata, P. Paravidino, D. Perdicchia, C. Giannini, M. Bencini, K. Clays and A. Persoons, *Tetrahedron*, 2003, **59**, 6481-6488.
49. M. H. Garcia, P. Florindo, M. d. F. M. Piedade, S. Maiorana and E. Licandro, *Polyhedron*, 2009, **28**, 621-629.
50. H.-J. Son, W.-S. Han, D.-H. Yoo, K.-T. Min, S.-N. Kwon, J. Ko and S. O. Kang, *J. Org. Chem.*, 2009, **74**, 3175-3178.
51. H. Sakai, S. Shinto, Y. Araki, T. Wada, T. Sakanoue, T. Takenobu and T. Hasobe, *Chem. Eur. J.*, 2014, **20**, 10099-10109.
52. K.-T. Lin, H.-M. Kuo, H.-S. Sheu and C. K. Lai, *Tetrahedron*, 2014, **70**, 6457-6466.
53. A. D. Becke, *J. Chem. Phys.*, 1993, **98**, 5648.
54. M. Caricato, G. W. Trucks and M. J. Frisch, *J. Chem. Theory Comput.*, 2010, **6**, 1966-1970.
55. C.-G. Liu, X.-H. Guan and Z.-M. Su, *J. Phys. Chem. C*, 2011, **115**, 6024-6032.
56. S. Grimme and S. D. Peyerimhoff, *Chem. Phys.*, 1996, **204**, 411-417.
57. P. A. Brooksby and W. R. Fawcett, *Spectrochim. Acta, Part A*, 2001, **57**, 1207-1221.
58. C. Bernini, L. Zani, M. Calamante, G. Reginato, A. Mordini, M. Taddei, R. Basosi and A. Sinicropi, *J. Chem. Theory Comput.*, 2014, **10**, 3925-3933.
59. C. J. Cramer and D. G. Truhlar, *Chem. Rev.*, 1999, **99**, 2161-2200.
60. F. Mançois, L. Sanguinet, J.-L. Pozzo, M. Guillaume, B. Champagne, V. Rodriguez, F. Adamietz, L. Ducasse and F. Castet, *J. Phys. Chem. B* 2007, **111**, 9795-9802.
61. A. Plaquet, M. Guillaume, B. Champagne, F. Castet, L. Ducasse, J.-L. Pozzo and V. Rodriguez, *Phys. Chem. Chem. Phys.*, 2008, **10**, 6223-6232.
62. R. Bersohn, *J. Chem. Phys.*, 1966, **45**, 3184.
63. G. Kresse and J. Furthmüller, *Phys. Rev. B*, 1996, **54**, 11169-11186.
64. G. Kresse and J. Hafner, *Phys. Rev. B*, 1993, **48**, 13115-13118.
65. Y. L. Si, G. C. Yang and Z. M. Su, *J. Mater. Chem. C*, 2013, **1**, 1399.
66. Y. L. Si and G. C. Yang, *J. Phys. Chem. A*, 2014, **118**, 1094-1102.
67. Y. M. Sang, L. K. Yan, N. N. Ma, J. P. Wang and Z. M. Su, *J. Phys. Chem. A*, 2013, **117**, 2492-2498.
68. Y. L. Si and G. C. Yang, *RSC Adv.*, 2013, **3**, 2241-2247.
69. Y. M. Sang, L. K. Yan, J. P. Wang and Z. M. Su, *J. Phys. Chem. A*, 2012, **116**, 4152-4158.
70. H. Lee, S. Cheon and M. Cho, *J. Chem. Phys.*, 2010, **132**, 225102.
71. J. P. Wang, L. K. Yan, G. C. Yang, W. Guan and Z. M. Su, *J. Mol. Graphics Modell.*, 2012, **35**, 49-56.
72. I. Valencia, Y. Ávila-Torres, N. Barba-Behrens and I. L. Garzón, *J. Mol. Struct.*, 2015, **1085**, 52-62.
73. L. Li, B.-B. Yang and Y.-K. Si, *Chin. Chem. Lett.*, 2014, **25**, 1586-1590.
74. J. M. Slocik, A. O. Govorov and R. R. Naik, *Nano Lett.*, 2011, **11**, 701-705.
75. S. Grimme, J. Harren, A. Sobanski and F. Vögtle, *Eur. J. Org. Chem.*, 1998, **1998**, 1491-1509.
76. A. Rauk, D. Yang, D. Tsankov, H. Wieser, Y. Koltypin, A. Gedanken and G. V. Shustov, *J. Am. Chem. Soc.*, 1995, **117**, 4160-4166.
77. G. V. Shustov, A. V. Kachanov, G. K. Kadorkina, R. G. Kostyanovskii and A. Rauk, *J. Am. Chem. Soc.*, 1992, **114**, 8257-8262.
78. G. V. Shustov, S. V. Varlamov, I. I. Chervin, A. E. Aliev, R. G. Kostyanovskii, D. Kim and A. Rauk, *J. Am. Chem. Soc.*, 1989, **111**, 4210-4215.
79. A. E. Hansen and T. D. Bouman, *J. Am. Chem. Soc.*, 1985, **107**, 4828-4839.
80. J. Morcellet-Sauvage, M. Morcellet and C. Loucheux, *Macromolecules*, 1984, **17**, 452-456.
81. C. R. Legler, N. R. Brown, R. A. Dunbar, M. D. Harness, K. Nguyen, O. Oyewole and W. B. Collier, *Spectrochim. Acta, Part A*, 2015, **145**, 15-24.
82. E. Miliordos and S. S. Xantheas, *J. Chem. Phys.*, 2015, **142**, 094311.

83. B. G. Janesko and D. Yaron, *J. Chem. Theory Comput.*, 2005, **1**, 267-278.
84. G. I. Csonka, A. Ruzsinszky and J. P. Perdew, *J. Phys. Chem. B*, 2005, **109**, 21471-21475.
85. E. A. Bushnell and R. J. Boyd, *J. Phys. Chem. A*, 2015, **119**, 911-918.
86. E. Geidel and F. Billes, *J. Mol. Struct. (Theochem)*, 2000, **507**, 75-87.
87. N. Ramos-Berdullas, I. Perez-Juste, C. Van Alsenoy and M. Mandado, *Phys. Chem. Chem. Phys.*, 2015, **17**, 575-587.
88. A. Neugebauer and G. Häfelinger, *J. Mol. Struct. (Theochem)*, 2002, **578**, 229-247.
89. A. Slimani, X. Yu, A. Muraoka, K. Boukheddaden and K. Yamashita, *J. Phys. Chem. A*, 2014, **118**, 9005-9012.
90. M. D. Wodrich, C. Corminboeuf and P. v. R. Schleyer, *Org. Lett.*, 2006, **8**, 3631-3634.
91. C. Lepetit, H. Chermette, M. Gicquel, J.-L. Heully and R. Chauvin, *J. Phys. Chem. A*, 2007, **111**, 136-149.
92. A. Forni, S. Pieraccini, S. Rendine and M. Sironi, *J. Comput. Chem.*, 2014, **35**, 386-394.
93. F. Moscardó and A. J. Pérez-Jiménez, *Int. J. Quantum. Chem.*, 1998, **67**, 143-156.
94. D. Jacquemin and C. Adamo, *Int. J. Quantum. Chem.*, 2012, **112**, 2135-2141.
95. R. Gayathri and M. Arivazhagan, *Spectrochim. Acta, Part A*, 2014, **123**, 309-326.
96. D. Mahadevan, S. Periandy and S. Ramalingam, *Spectrochim. Acta, Part A*, 2011, **84**, 86-98.
97. N. X. Wang and A. K. Wilson, *J. Phys. Chem. A*, 2003, **107**, 6720-6724.
98. J.-L. Chen, J.-T. Hong, K.-J. Wu and W.-P. Hu, *Chem. Phys. Lett.*, 2009, **468**, 307-312.
99. E. G. Hohenstein, S. T. Chill and C. D. Sherrill, *J. Chem. Theory Comput.*, 2008, **4**, 1996-2000.
100. B. S. Jursic, *J. Mol. Struct. (Theochem)*, 1998, **432**, 211-217.
101. W.-T. Chan, I. P. Hamilton and H. O. Pritchard, *J. Chem. Soc., Faraday Trans.*, 1998, **94**, 2303-2306.
102. R. Orlando, V. Lacivita, R. Bast and K. Ruud, *J. Chem. Phys.*, 2010, **132**, 244106.
103. S. Tomić and N. M. Harrison, *AIP Conference Proceedings*, 2010, **1199**, 65-66.
104. N. Kuritz, T. Stein, R. Baer and L. Kronik, *J. Chem. Theory Comput.*, 2011, **7**, 2408-2415.
105. B. M. Wong and T. H. Hsieh, *J. Chem. Theory Comput.*, 2010, **6**, 3704-3712.
106. F. Furche and R. Ahlrichs, *J. Chem. Phys.*, 2001, **114**, 10362.
107. G. C. Yang, Y. L. Si and Z. M. Su, *J. Phys. Chem. A*, 2011, **115**, 13356-13363.
108. E. Botek, J.-M. André, B. Champagne, T. Verbiest and A. Persoons, *J. Chem. Phys.*, 2005, **122**, 234713.
109. M. Kauranen, T. Verbiest and A. Persoons, *Journal of Nonlinear Optical Physics & Materials*, 1999, **08**, 171-189.
110. Y. Zhang and B. Champagne, *J. Phys. Chem. C*, 2012, **116**, 21973-21981.
111. A. Mahmood, M. I. Abdullah and M. F. Nazar, *Bull. Korean Chem. Soc.* , 2014, **35**, 1391-1396.
112. Y. Z. Li, Y. H. Zhang, D. W. Qi, C. F. Sun and L. P. Yang, *J. Mater. Sci. - Mater. Electron.*, 2014, **25**, 5255-5263.
113. F. Castet, A. Pic and B. Champagne, *Dyes and Pigments*, 2014, **110**, 256-260.
114. L. J. Zhang, D. D. Qi, L. Y. Zhao, C. Chen, Y. Z. Bian and W. J. Li, *J. Phys. Chem. A* 2012, **116**, 10249-10256.
115. L.-H. Zhang, Y. Wang, F. Ma and C.-G. Liu, *J. Organomet. Chem.*, 2012, **716**, 245-251.
116. G. C. Yang, Y. L. Si and Z. M. Su, *Org. Biomol. Chem.*, 2012, **10**, 8418-8425.
117. J. S. Chappell, A. N. Bloch, W. A. Bryden, M. Maxfield, T. O. Poehler and D. O. Cowan, *J. Am. Chem. Soc.*, 1981, **103**, 2442-2443.
118. D. R. Kanis, M. A. Ratner and T. J. Marks, *Chem. Rev.*, 1994, **94**, 195-242.
119. T. Hatakeyama, S. Hashimoto, T. Oba and M. Nakamura, *J. Am. Chem. Soc.*, 2012, **134**, 19600-19603.
120. T. H. Huang, W. T. Whang, J. Y. Shen, Y. S. Wen, J. T. Lin, T. H. Ke, L. Y. Chen and C. C. Wu, *Adv. Funct. Mater.*, 2006, **16**, 1449-1456.
121. Y. T. Yang, H. Geng, S. W. Yin, Z. G. Shuai and J. B. Peng, *J. Phys. Chem. B*, 2006, **110**, 3180-3184.
122. J. Widany, G. Daminelli, A. Di Carlo, P. Lugli, G. Jungnickel, M. Elstner and T. Frauenheim, *Phys. Rev. B*, 2001, **63**, 233204.
123. M. C. R. Delgado, E.-G. Kim, D. A. d. S. Filho and J.-L. Bredas, *J. Am. Chem. Soc.*, 2010, **132**, 3375-3387.
124. C. L. Li, S. P. Wang, W. P. Chen, J. B. Wei, G. C. Yang, K. Q. Ye, Y. Liu and Y. Wang, *Chem. Commun.*, 2015, DOI: 10.1039/C5CC03492B.
125. G. C. Yang, Y. Liao, Z. M. Su, H. Y. Zhang and Y. Wang, *J. Phys. Chem. A*, 2006, **110**, 8758-8762.